DOI: 10.1002/chem.201202213

A New Signal-On Photoelectrochemical Biosensor Based on a Graphene/Quantum-Dot Nanocomposite Amplified by the Dual-Quenched Effect of Bipyridinium Relay and AuNPs

Xiaoru Zhang,[a] Yunpeng Xu,[a] Yanqiang Yang,[b] Xia Jin,[a] Sujuan Ye,[a] Shusheng Zhang,*[a] and Lilin Jiang[b]

Abstract: A new photoelectrochemical (PEC) biosensor was developed by using carboxyl-functionalized graphene and CdSe nanoparticles. This sensitive interface was then successfully applied to detection of thrombin based on the dual-quenched effect of PEC nanoparticle, which relied on the electron transfer of a bipyridinium relay and energy transfer of AuNPs. After recognition with an aptamer, the PEC nanoparticle was removed and a signal-on PEC biosensor was obtained. Moreover, the bio-barcode technique used in the preparation of PEC nanoparticle could avoid cross-reaction and enhances the sensitivity. Taking advantages of the various methods mentioned above, the sensitivity could be easily enhanced. In addition, in this work we also investigated graphene that was modified with different functional groups and AuNPs of different particle sizes. Under optimal conditions, a detection limit of 5.9×10^{-15} M was achieved. With its simplicity, selectivity, and sensitivity, this strategy shows great promise for the fabrication of highly efficient PEC biosensors.

Keywords: biosensors · electron transfer · energy transfer · graphene · nanoparticles

Introduction

The photoelectrochemical detection method is a newly developed and promising analytical method for a biological assay.[1] By using photoirradiation coupled with electrochemical detection, the photoelectrochemical sensor is very sensitive with low background signals. Photoelectrochemically active species that are usually used are rutheniumbipyridine derivatives,[2,3] semiconductor nanostructures (such as CdSe/CdS,[4] TiO_2 [5] and ZnO[6]), and dyes.[7] Among them, semiconductor nanoparticles (NPs) have attracted much attention, due to the unique size- and shape-dependent optical and electronic properties. The photochemical excitation of semiconductor NPs to form an electron–hole pair is the primary event for the photocurrent generation. However, the transfer of conduction-band electrons to the electrode is hampered by the competing electron–hole recombination process. Hence, some strategies have been attempted including the introduction of nanomaterials with a suitable band energy as efficient acceptors.[8,9]

Graphene, as an atomic-layer-thick 2D system, has triggered considerable research interests owing to its unique optical, electronic, thermal, and mechanical properties. These fascinating properties of graphene hold promising potential for electronic devices, sensitive chemical sensors, thermal management, and composite materials.[10,11] Recently, Chen et al.[11] has reviewed the applications of graphene in organic photovoltaic (OPV) cells, including transparent electrodes, active layers, and interface layers. As a good candidate for the acceptor material in OPV applications, graphene has large donor/acceptor interfaces for charge generation and a continuous pathway for electron transfer. The groups of Lin[12] and Li[13] have reported quantum dot (QD)-sensitized graphene heterostructures prepared by in situ growth of QDs on graphene, and applied them to construct QD-sensitized photoelectrochemical cells. Geng et al.[10] has fabricated composite films through the noncovalent coupling of CdSe QDs to graphene for flexible and transparent optoelectronic films. Guo et al.[14] have prepared layered graphene/quantum dots for photovoltaic devices. Zhu and coworkers[15] have prepared a graphene–CdS composite in a one-step synthesis, which was then used for the fabrication of a photoelectrochemical cytosensor by using a layer-by-layer assembly process. Our group has prepared a photoelectrochemical biosensor based on functionalized graphene and CdSe nanoparticles multilayers.[16] In all these studies, QD–graphene composites were prepared by in situ growth,

[a] Dr. X. Zhang, Y. Xu, X. Jin, S. Ye, Prof. S. Zhang
Key Laboratory of Biochemical Analysis
Ministry of Education, College of Chemistry and Molecular Engineering
Qingdao University of Science and Technology
Qingdao 266042 (P.R. China)
Fax: (+86) 532-84022750
E-mail: shushzhang@126.com

[b] Prof. Y. Yang, Dr. L. Jiang
Center for Condensed Matter Science and Technology
Department of Physics, Harbin Institute of Technology
Harbin 150001 (P.R. China)

Supporting information for this article is available on the WWW under http://dx.doi.org/10.1002/chem.201202213.

physical adsorption and chemical modification. It is expected that the chemical modification could not only enhance its solubility and processability, but also render new properties to graphene and even greatly widen its application scope. Thus, developing chemical methods to functionalize graphene has become critical in the further exploitation of graphene technologies. In this paper, a bifunctional compound with azide groups at one end and carboxyl group at the other end was utilized to prepare carboxyl-functionalized graphene by using nitrene cycloaddition.[17] The resulting functionalized graphene nanosheets are electrically conductive, readily dispersible in solvents and easily processable, making them excellent candidates for further modification with QD.

A graphene–QD nanocomposite was assembled for the construction of the photoelectrochemical biosensor. Photocurrent variation was produced prior to and after the biorecognition event. In terms of signal changes, sensors could be classified into two types: signal-off and signal-on. In the case of a signal-off photoelectrochemical biosensor, the recognition of proteins on the modified electrode generate a hydrophobic layer and thus partly hinder the diffusion of a sacrificial electron-donor to the surface of CdS or CdSe QDs, which lead to a decrease of photocurrent. So far, most photoelectrochemical biosensors developed belong to this kind.[15,18–20] However, these signal-off sensors suffer from false positives when photoactive species become degraded and are limited in their signal gain because the target can suppress no more than 100% of the original signal.[21,22] In this regard, signal-on sensors are highly deserved.

The photoinduced electron-transfer between semiconductor nanoparticle and *N*,*N*′-dimethyl-4,4′-bipyridinium (V^{2+}) salts has attracted a great deal of attention by the group of Willner.[23,24,25] The concept of vectorial electron-transfer was adopted in semiconductor nanoparticle systems. When the CdS NPs are located close to the electrode and positioned between the relay units V^{2+} and electrode through the hybridization of template DNA, the photocurrent that is measured is substantially lower than the photocurrent measured in the presence of the CdS NPs alone. This implies that the bipyridinium acceptor units can act as conduction-band electron traps. Besides photoinduced electron-transfer of bipyridinium, AuNPs have been widely utilized in bioaffinity sensors due to their physical properties. It is well known that when CdS QDs and AuNPs are in close proximity under certain conditions, a unique phenomenon of interparticle energy-transfer will occur.[26–28] Recently, Xu and co-workers[29] have reported the energy transfer between CdS QDs and AuNPs in a PEC detection system and a sensitive biosensing of DNA was realized based on this mechanism.

In this study, we report an efficient method to fabricate a signal-on PEC sensor. Carboxyl-functionalized graphene was synthesized to construct a CdSe QD-sensitized graphene PEC-sensing interface. The dual-quenched PEC film, achieved by electron transfer of a bipyridinium relay and energy transfer of AuNPs, largely lowered the initial signal. After removal of bipyridinium relay and AuNPs through a biorecognition event, significant signal restore could be obtained. By integrating the signal amplification effect of functionalized graphene and the dual-quenched effect of bipyridinium relay and AuNPs in a conventional analytical strategy, thrombin could be sensitively detected. Furthermore, this work opens up the possibility for designing more efficient PEC biosensors.

Results and Discussion

Principle of the assay for the detection of thrombin: The fabrication of the sensing design is shown in Scheme 1. First-

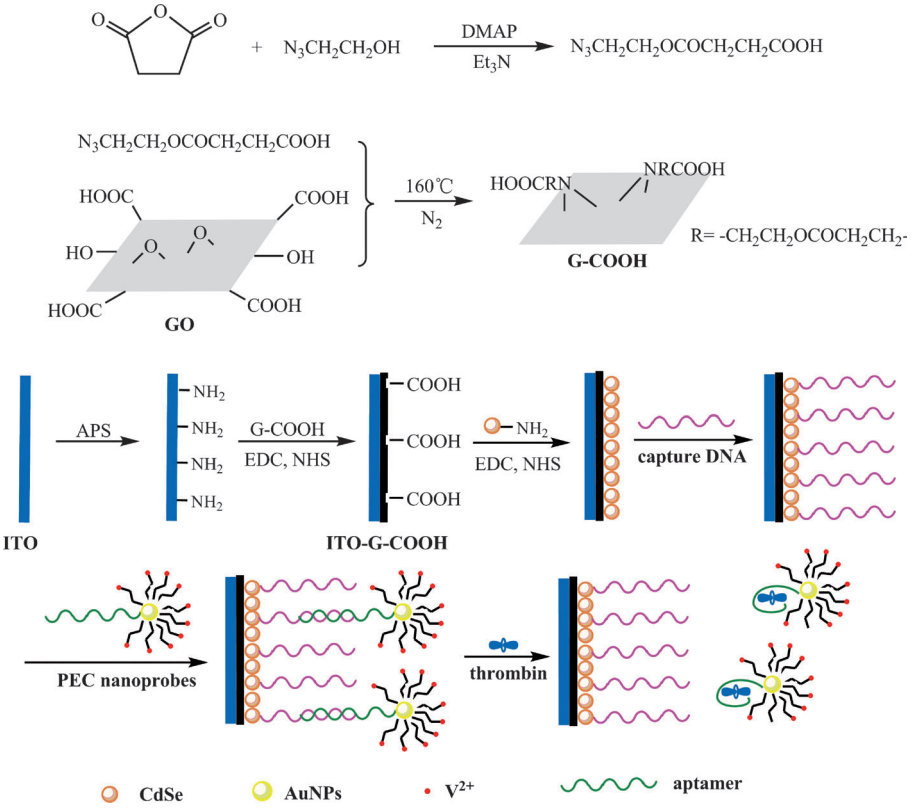

Scheme 1. Schematic diagram for preparation of carboxyl-functionalized graphene and the fabrication of amplified signal-on thrombin biosensor.

ly, the carboxyl-functionalized graphene was synthesized based on nitrene chemistry.[16,30] 4-(2-azidoethoxy)-4-oxobutanoic acid, which contains both azido and carboxyl groups in one molecule, was prepared by the acylation of succinic anhydride with 2-azidoethanol. Then, the azido group was anchored onto graphene by an electrophilic [2+1] cycloaddition to afford the aziridine rings. The left carboxyl group extended into the surrounding solvent to solubilize graphene and could be used for further chemical modification. Secondly, the indium tin oxide (ITO) electrode was silanized with aminopropyltriethoxysilane (APS) and then the carboxyl-functionalized graphene was assembled onto an amino-functioned electrode through an amide bond. Then, CdSe-NH_2 NPs was also assembled on the surface graphene through an amide bond to give the photoactive film. The PO_3H groups that were used to modify the capture DNA were covalently bound to the CdSe NPs by using the classic coupling reactions between $-NH_2$ groups on the surfaces of CdSe NPs and $-PO_3H$ groups of DNA. Finally, the capture DNA underwent hybridization with the thrombin aptamer on PEC nanoprobes, which contained V^{2+} and the aptamer on the bio-barcode of AuNPs. The photocurrent was reduced due to the introduction of AuNPs and V^{2+} to the surface of electrode. After recognition of thrombin by the aptamer, the PEC nanoprobes were removed and the photocurrent was enhanced accordingly. Thus, a signal-on PEC biosensor for the detection of thrombin was obtained.

Characterization of graphene and the CdSe NP-modified ITO electrode and the performance of composite material: To confirm that the successful assembly of graphene and CdSe NPs on ITO electrode, SEM was performed and the images were generated. Figure 1 A is a typical SEM image of G-COOH assembled on an APS-modified ITO electrode, showing that the functionalized graphene has a sheet-like morphology with a clear, smooth surface. Figure 1 B shows the SEM image of the composite film, in which the CdSe–NH_2 NPs were attached to the graphene. The NPs uniformly distributed on graphene, evidencing the well-behaved assembly process.

To verify the amplification effect of graphene on the photocurrent, the photocurrents generated by graphene, CdSe-QDs and QD-sensitized graphene on ITO electrodes were measured under the same conditions. As demonstrated in curve (c) of Figure 2, the QD-sensitized graphene photoelectrode generated photocurrent at about 1.65 μA, whereas the control experiments showed no significant photocurrent generation by graphene-modified ITO (curve a) and only about 520 nA for the pure CdSe-QD-modified ITO electrode (curve b), which indicated the enhancing ability of graphene. This could be explained by two aspects: Firstly, the two-dimensional sheet morphology of graphene provided a large surface area for QD-loading, which facilitated the carrying of more photoactive QDs and capturing more light. Secondly, the electron-accepting ability of graphene might contribute to the enhancement of electron transport and thus impede the charge recombination of excited CdSe.[8,15]

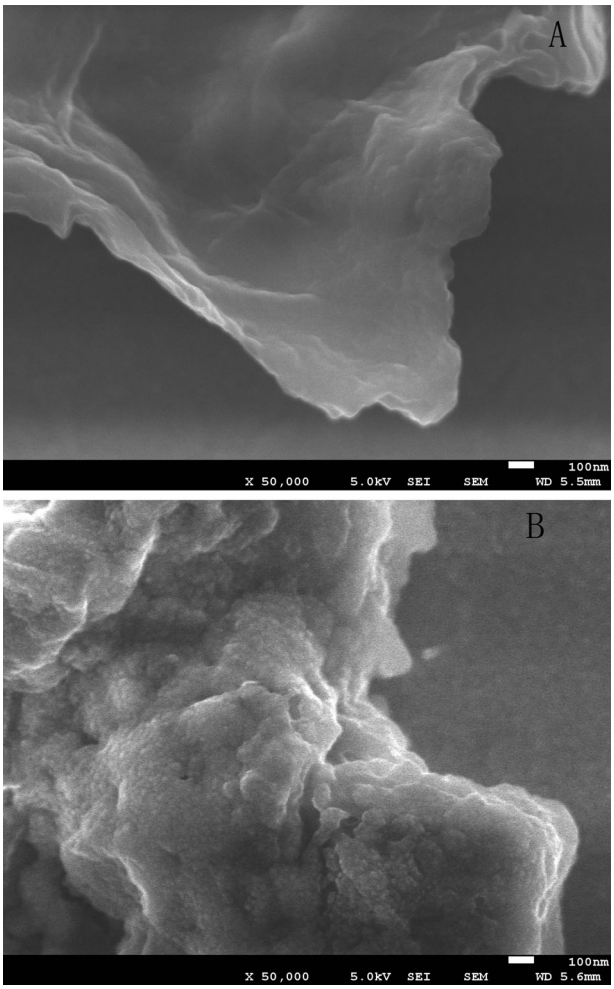

Figure 1. SEM images of A) G-COOH and B) G-COOH/CdSe composite film on the ITO electrode.

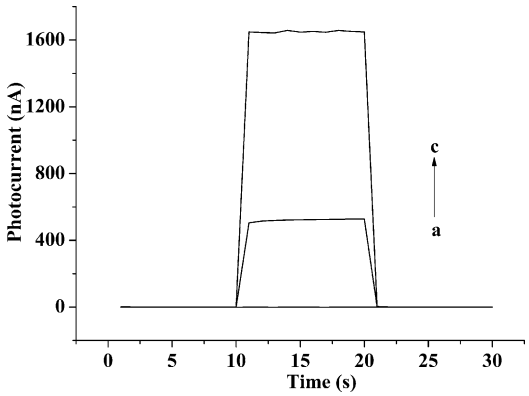

Figure 2. Photocurrent responses for a) G-COOH; b) CdSe-NH_2 QDs; c) G-COOH and CdSe-NH_2 QD-modified ITO electrodes.

The photoluminescence (PL) spectra were also used to illustrate the role of graphene. The PL spectra of pure CdSe–NH_2 NPs solution and the graphene-CdSe NPs mixture were measured. As can be seen in Figure 3, a dominant emission peak at 549 nm could be clearly observed for the pure

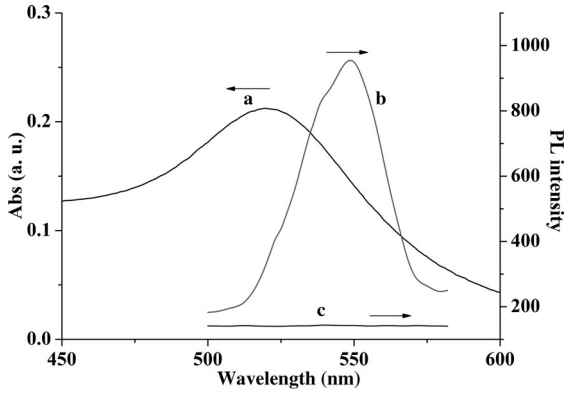

Figure 3. Absorption spectrum of a) AuNPs as well as the corresponding PL spectra (excited at 400 nm) of b) pure CdSe NPs and c) graphene-CdSe NPs mixture.

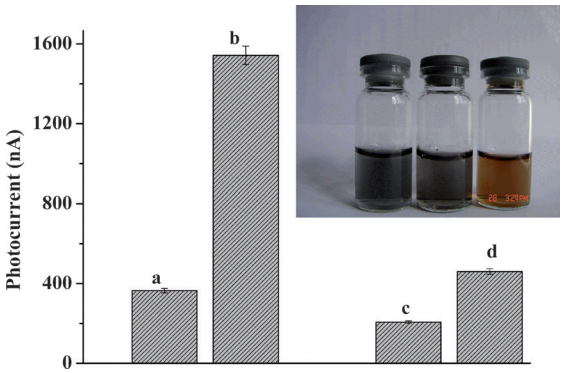

Figure 4. Photocurrent value for a) CdSe-NH_2; b) CdSe-NH_2/G-COOH; c) CdSe-COOH; d) CdSe-COOH/G-NH_2-modified Au electrode. Inset from left to right: Photographs of G-COOH, G-NH_2, and GO dispersed in water.

CdSe-NH_2 NPs (red), whereas the PL of graphene-CdSe NPs mixture is too weak to be identified (blue). The significantly quenched PL can be attributed to the fact that the photoinduced electrons and holes in the CdSe NPs prefer separately transferring to the graphene and electron–hole pairs recombination of CdSe NPs is hampered.[12]

Chemical modification could not only enhance its solubility and processability, but also render new properties to graphene. The properties of graphene may be different when it is modified through various methods. Here we compared the photoelectrochemical interface made from carboxyl-modified graphene (G-COOH, inset of Figure 4A) with amino-modified graphene (G-NH_2, insert of Figure 4B), which was assembled with an amino- or carboxyl group-modified CdSe QD, respectively. This contrast experiment was carried out on planar Au electrode for easy assembly (for the preparation process see the Supporting Information). As shown from Figure 4, the photocurrent of CdSe–NH_2 QD alone was 364 nA. After assembly with G-COOH, the photocurrent increased to 1.54 μA. Nevertheless, the enhancement effect for G-NH_2 to CdSe-COOH was not as distinct as the former. The excellent solubility of G-COOH compared with G-NH_2 is an important factor for the improved performance of G-COOH.

Photoinduced electron-transfer effect of viologen: MV^{2+} is widely used as an electron acceptor in molecular and nanoparticle systems. From previous work,[31,32] the electrons accumulated within the conduction band of the CdSe (E_{CB} = −0.6 V vs NHE)[33] are energetic enough to transfer to MV^{2+} ($E^0(MV^{2+}/MV^{+\bullet})$ = −0.445 V vs. NHE).[34,35] The photoinduced reactions between CdSe and MV^{2+} are summarized in Equations (1)–(4) in which $h\nu$ is photon energy, h and e represent holes and electrons, respectively, and h_t represents shallow and deep-trap holes..[31]

$$\mathrm{CdSe} + h\nu \rightarrow \mathrm{CdSe} + (\mathrm{h} + \mathrm{e}) \quad (1)$$

$$\mathrm{CdSe}\ (\mathrm{h} + \mathrm{e}) \rightarrow \mathrm{CdSe} + h\nu' \quad (2)$$

$$\mathrm{CdSe}\ (\mathrm{h} + \mathrm{e}) + \mathrm{MV}^{2+} \rightarrow \mathrm{CdSe}\ (\mathrm{h_t}) + \mathrm{MV}^{+\bullet} \quad (3)$$

$$\mathrm{CdSe}\ (\mathrm{h_t}) + \mathrm{MV}^{+\bullet} \rightarrow \mathrm{CdSe} + \mathrm{MV}^{2+} \quad (4)$$

The study of photoinduced electron-transfer effect of viologen and its usage in the detection of thrombin was described in Scheme 2 and the change of photocurrent during each step was described in Figure 5A. For G-COOH/CdSe-NH_2 nanocomposite film on ITO, as described earlier, a large photocurrent was observed (1.65 μA, curve c). When capture DNA was covalently attached on CdSe NPs, the photocurrent was increased further (1.98 μA, Figure 5A; curve d). Then, the photocurrent decreased after the bipyridinium-functionalized aptamer nucleic acid hybridized with the capture DNA template (Figure 5A; curve a, 1.28 μA). This result could be explained by the fact that in addition to the ejection of the conduction-band electrons to the electrode, the other competitive electron-transfer path that exists involves the ejection of the photoexcited conduction-band electrons to the bipyridinium relay (see Figure 5B). The net photocurrent in the system is the result of the oppositely directed photocurrents.[23,24] Finally, after the recognition of aptamer DNA with 1.0×10^{-11} M thrombin, the photocurrent was restored to about 1.54 μA for the removal of bipyridinium (Figure 5A; curve b).

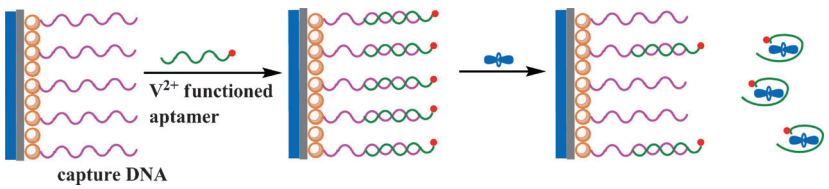

Scheme 2. Schematic diagram for the detection of thrombin based on the photoinduced electron-transfer effect of viologen alone.

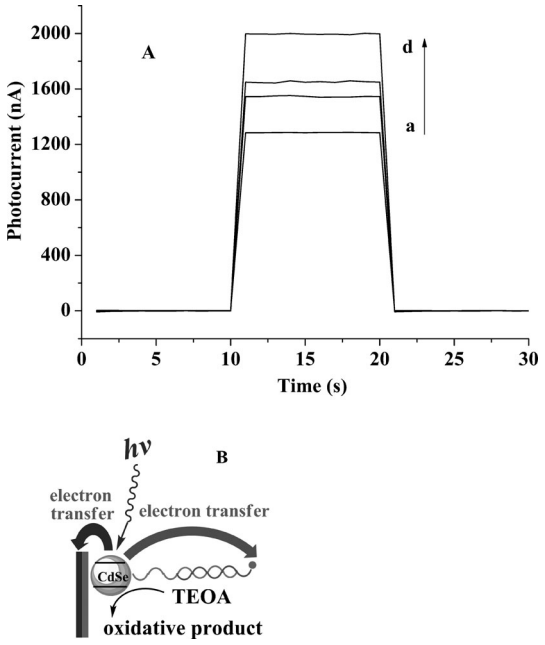

Figure 5. A) Photocurrent responses for a) ITO/G-COOH/CdSe/capture DNA/V^{2+}; b) ITO/G-COOH/CdSe/capture DNA/V^{2+}/1.0×10^{-11} M thrombin; c) ITO/G-COOH/CdSe; d) ITO/G-COOH/CdSe/capture DNA. B) Schematic diagram for the direction of photocurrent under the action of V^{2+}.

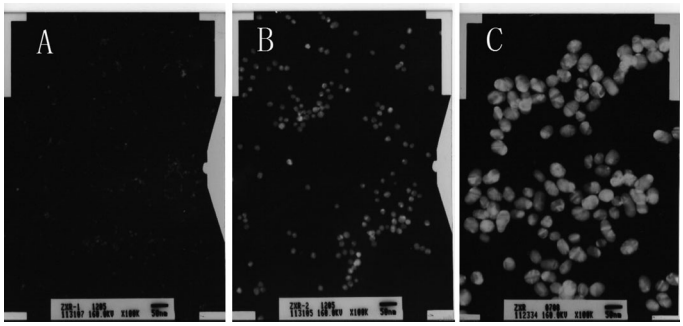

Figure 6. TEM images of A) AuNPs: 5 nm, B) AuNPs: 18 nm, and C) AuNPs: 45 nm.

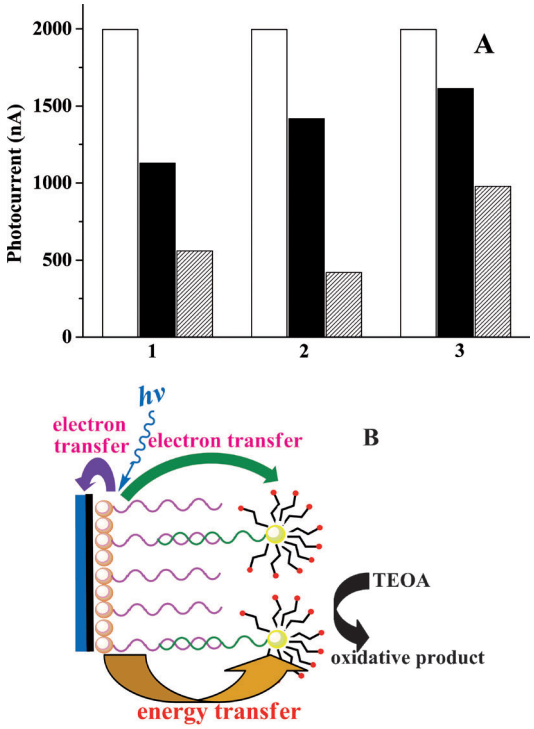

Figure 7. A) Photocurrent value of different particle sizes. **1**, **2**, and **3** represent the photocurrent response of particles of sizes 5, 18, and 45 nm, respectively. White columns represent the original photocurrent without AuNPs and V^{2+}. The black columns indicate the value of the photocurrent after introducing AuNPs alone. The gray columns represent the photocurrent after introducing PEC nanoprobes, which contained both AuNPs and V^{2+}. B) Schematic diagram for the direction of photocurrent under the action of PEC nanoprobes.

Energy transfer between CdSe QDs and AuNPs: Recently, Xu and co-workers have reported that when CdS QDs and AuNPs have a larger interparticle distance in a PEC system, a unique phenomenon of interparticle energy transfer occurs.[29] Herein, the PL- and UV/Vis absorption spectra were analyzed to verify this phenomenon. As shown in Figure 3, the PL spectrum of the prepared CdSe QDs, whose main peak centered at 549 nm and shoulder peak centered at 537 nm, was observed with excitation wavelength of 400 nm (red). However, the UV/Vis absorption spectrum of AuNPs observed at 520 nm (black) has a large spectral overlap with the emission spectrum of the CdSe QDs. So, energy transfer between CdSe QDs and AuNPs could lead to the reduction of photocurrents produced by the film of CdSe QDs.

The role of AuNPs in this design is two-fold: First, it can serve as carrier, supporting relay viologen through cysteamine. Second, the presence of AuNPs can cause energy transfer, which leads to a further decrease of the photocurrent. Here we prepared the AuNPs in three different sizes (5, 18, and 45 nm; for preparation see the Supporting Information). TEM images of prepared AuNPs showed regular shape and homogeneous distribution (Figure 6). The influence of different particle size on the depression of the photocurrent was investigated in Figure 7A. Comparing the white and black columns, the decrease in the photocurrent was 43.5, 29, and 19.2%, respectively, for the differently sized AuNPs (5, 18, and 45 nm); the optimal energy-transfer efficiency was produced by 5 nm AuNPs. After incorporating V^{2+}, the decrease of photocurrents produced by PEC nanoprobes was 72, 79 and 51%, respectively; however, this might be caused by the high-loading capacity of bigger AuNPs. Taking these factors into account, 18 nm AuNPs were used in following experiment. The influence of PEC nanoprobes to photocurrent is illustrated in Figure 7B. By incorporating the electron-transfer effect of the bipyridinium relay and energy-transfer effect of AuNPs, the photocurrent was reduced significantly.

Sensitivity: An aptamer can bind tightly and specifically to its target molecules with a binding constant greater than that of an ordinary double-stranded DNA. So, when the assembled electrode ITO/graphene/CdSe/AuNPs/V^{2+} was added to a solution containing thrombin, the double helixes were opened and the PEC nanoprobes were detached from the surface of electrode, which led to the increase of photocurrents to produce a signal-on photoelectrochemical biosensor. Figure 8A showed the photocurrent signals that

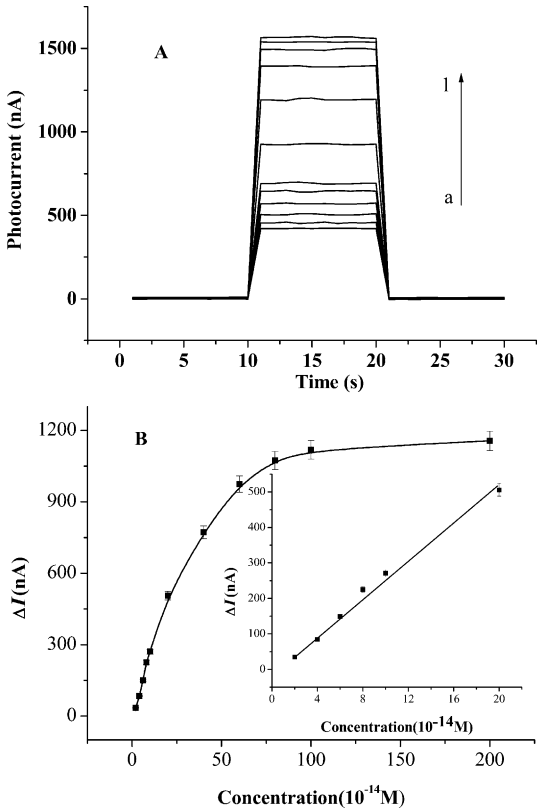

Figure 8. A) Photocurrent responses for different concentrations of thrombin (in M): a) 0, b) 2.0×10^{-14}, c) 4.0×10^{-14}, d) 6.0×10^{-14}, e) 8.0×10^{-14}, f) 1.0×10^{-13}, g) 2.0×10^{-13}, h) 4.0×10^{-13}, i) 6.0×10^{-13}, j) 8.0×10^{-13}, k) 1.0×10^{-12}, l) 2.0×10^{-12}. B) Calibration curve corresponding to the analysis of different concentration of thrombin from 2.0×10^{-14} to 2.0×10^{-12} M. Inset: the linear range from 2.0×10^{-14} to 2.0×10^{-13} M.

were responsive to the changing concentrations of thrombin (a–l). The photocurrent intensity gradually increased with increasing thrombin concentrations. As shown in Figure 8B, the increase of photocurrent intensity was linearly related to the concentration of thrombin ($c_{thrombin}$) in the range from 2.0×10^{-14} to $\approx2.0\times10^{-13}$ M. The regression equation was ΔI (nA) $= -6.25 + 26.39\, c_{thrombin}(10^{-14}\,M)$ with a regression coefficient of 0.9982. The relative standard deviation for 11 repetitive measurements of 6.0×10^{-14} M was 4.3%, and the limit of quantification (LOQ) was 2.0×10^{-14} M (10σ) under the optimum conditions. With the amplification by AuNPs, the sensitivity of the proposed method was enhanced about 100-fold compared with a simple photoelectrochemical detection based on V^{2+} (see Figure S3 in the Supporting Information).

Selectivity: Control experiments were conducted to reveal the specificity of the recognition reaction for thrombin. As seen in Figure 9, when thrombin (1.0×10^{-13} M) was added,

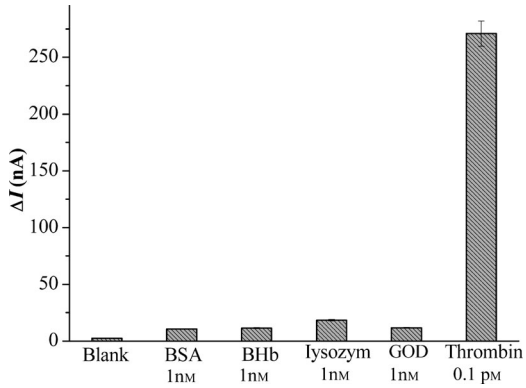

Figure 9. The selectivity of thrombin toward different analytes.

the photocurrent increased by 270 nA. However, no obvious photocurrent change was detected when the aptamer was treated with foreign proteins, such as bovine serum albumin (BSA), hemoglobin (BHb), lysozyme, and glucose oxidase (GOD), even with concentrations of 10^4-fold excess. This may be explained by the specific binding between the target and the aptamer.

Conclusion

We have prepared a new composite material interface through a simple approach and developed a signal-on PEC biosensor based on dual-quenched mechanism. Several advantages of our method have been demonstrated: 1) Carboxyl-functionalized graphene was prepared and used as a good candidate for the collection and transport of photogenerated charges of CdSe NPs for the first time. Such composite material interface possesses higher sensitivity and is promising as a PEC biosensor. 2) Compared with the conventional signal quenching PEC biosensors, a signal-on PEC assay was developed that could avoid false-positive results and enhance the accuracy of the result. 3) The dual-quenched PEC nanoparticle, achieved by electron transfer of bipyridinium relay and energy transfer of AuNPs, could largely reduce the initial signal before recognition of thrombin and improve the detection sensitivity greatly. 4) The specificity of a bio-barcode and the recognition of an aptamer were integrated in photoelectrochemical biosensor. In this way, improvement of selectivity and sensitivity could be easily achieved. So, with its simplicity, selectivity, and sensitivity, the present work details a promising new approach for highly efficient photoelectrochemical biosensors, which can expand the application scope of photoelectrochemistry, and has extensive potential in analytical applications.

Experimental Section

Materials: Sodium azide, iodomethane, succinic anhydride, triethylamine (Et_3N), 3-chloropropylamine hydrochloride, *N*,*N*-dimethyl formamide (DMF), *N*-methyl-2-pyrrolidinone (NMP), *N*,*N*-(dimethylamino)-pyridine (DMAP), 2-chloroethanol, and 4,4′-bipyridine were obtained from Sinopharm Chemical Reagent Co., Ltd. 3-aminopropyltriethoxysilane (APS), $HAuCl_4 \cdot 4H_2O$ (48%, w/w), ascorbic acid (AA), *N*-hydroxysuccinimide (NHS) and 1-(3-dimethylamino- propyl)-3-ethylcarbodiimide hydrochloride (EDC) were purchased from Aladdin's reagent (Shanghai) Co., Ltd. Glucose oxidase (GOD), bovine serum albumin (BSA), hemoglobin (BHb), and lysozyme were obtained from Sigma–Aldrich. Thrombin was obtained from Merck-chemicals. 2-Aminothanethiol (AET) and mercaptoacetic acid were purchased from ACROS Organics (Japan) and used as received.

All of synthetic oligonucleotides were purchased from SBS Genetech. Co. Ltd. (China). Their base sequences are as follows: capture DNA: 5′-PO_3H -TTT TTC CAA CCA CAC CAA CC-3′; thrombin aptamer: 5′-SH-TTT TTT GGT TGG TGT GGT TGG-3′.

Apparatus: The photocurrent was measured on an electrochemical workstation (Zahner Zennium, Germany). A three-electrode system was employed with Pt wire as an auxiliary electrode, Ag/AgCl as a reference electrode, and ITO conductive glass supplied by Weiguang Corp. (Shenzhen, People's Republic of China, ITO coating ((180 ± 25) nm, sheet resistance $\leq$ 10 Ω/square) as a working electrode. The planar Au electrode was supplied by Nanjing Research Institute of the fifty-fifth (2000 Å). Scanning electron microscopy (SEM) (JSM-6700F, JEOL, Japan) was used to examine the morphology of modified electrodes. Photoluminescence (PL) spectra were obtained on an RF-540 spectrophotometer (Shimadzu). UV/Vis spectra were carried out on a Cary 50 UV/Vis-NIR spectrophotometer (Varian).

Synthesis of PEC nanoprobes:[36] Tris-HCl (pH 8.2; 1.5 μL of 500 mM), TCEP (6 μL of 10 mM), -SH-modified thrombin aptamer (7.2 μL of 100 μM), and cysteamine (7.2 μL of 100 μM) were mixed and incubated for 30 min at room temperature. AuNPs (1 mL) (synthesized in Supporting Information) was added to the mixture and incubated for 6 h at room temperature. Then sodium boracic acid buffer (pH 9.0; 120 μL 0.1 M) and synthesized V-NHS (8 μL; see the Supporting Information) were added. The tube was placed on a shaking table for 10 h in dark. Then, the solution was centrifuged at 4 °C for 30 min at 10000 rpm and resuspended in buffer (800 μL of 100 mM NaCl, 25 mM Tris acetate, pH 8.2).

During the preparation of PEC nanoparticle, the molar ratio of cysteamine to aptamer DNA was optimized in Figure S6 (the Supporting Information).

Preparation of covalently functionalized graphene nanosheets:[17,30] Graphite oxide (GO) (50 mg) obtained by using the modified Hummers method[10,37] was dissolved in NMP (20 mL). The mixture was treated with an ultrasonic bath (40 kHz) for 1 h, then equipped with a condenser and placed on a magnetic stirrer with an oil bath. After bubbling with nitrogen for 30 min, Az-COOH (1.0 g) or Az-NH_2 (synthesized in the Supporting Information) was added. The reaction mixture was stirred at 160 °C for 18 h under a nitrogen atmosphere. After being cooled to room temperature, the mixture was separated by repeated centrifugation and washed with acetone. Next, the product was dried in vacuum oven to give G-COOH or G-NH_2. IR_{G-COOH} (KBr): $\tilde{\nu}$ = 2926, 2857 cm^{-1} (s); IR_{G-NH2} (KBr): $\tilde{\nu}$ = 2925, 2852 cm^{-1} (m); IR_{GO} (KBr): $\tilde{\nu}$ = 2922, 2850 cm^{-1} (w). These IR absorption frequencies are consistent with values reported in the Supporting Information of ref. [17].

Fabrication of the biosensor and thrombin analysis: The graphene-CdSe NPs composite film was prepared through amide link. Briefly, the ITO slices were sonicated in acetone, NaOH (1 M) in 1:1 (v/v) ethanol/water, and water, respectively, for about 15 min each. Then, the ITO slices were silanized in a solution of ethanol containing 2% APS for 12 h at room temperature. After this time, the electrode was rinsed with ethanol once and distilled water twice, then dried under an N_2 atmosphere.

PBS buffer (pH 7.4; 10 μL) containing G-COOH (0.5 mg mL^{-1}), NHS (0.005 M), and EDC (0.01 M) was casted on silanized-ITO electrode and incubated at room temperature for 12 h. After rinsing once with PBS and twice with distilled water, the electrode was dried under N_2 atmosphere, before CdSe-NH_2 NPs (10 μL; synthesis detailed in the Supporting Information) was casted on and incubated at room temperature for 2 h. The electrode was then washed twice with distilled water and dried under N_2 atmosphere to give the photoelectrochemically active interface.

Conjugation of capture DNA onto a CdSe nanoparticle-modified electrode was also achieved by using the classic EDC coupling reactions between NH_2 groups on the surfaces of the AET-capped CdSe NPs and the -PO_3H groups of capture DNA. Briefly, phosphate-modified capture DNA (20 μL, 10^{-5} M) was activated in imidazole buffer (pH 6.8; 40 μL, 0.1 M) containing EDC (40 μL, 0.2 M). Next, activated capture DNA (10 μL) was casted onto the surface of amino group modified electrode and incubated at room temperature overnight. After incubation, the electrode was rinsed with 0.4 M NaOH and 0.25% SDS solution to remove the free DNA.

PEC nanoprobes were assembled on electrode by hybridization between capture DNA and aptamer on nanoprobes. The nanoprobes (10 μL) obtained above were casted on the electrode and incubated at 37 °C for 2 h. Finally, the thrombin solutions (10 μL) were casted onto the surface of the modified electrode and incubated at room temperature for 0.5 h. The electrode surface was washed with distilled water twice and dried under N_2 atmosphere after each step of fabrication process.

PEC detection: Photoelectrochemical detection was carried out in PBS (pH 7.4, 0.1 M) containing 0.1 M ascorbic acid (AA) which was served as a sacrificial electron donor during the photocurrent measurement. Light excitation of 430 nm was switched every 10 s. The applied potential was 0.1 V.

Acknowledgements

This work was supported by the National Natural Science Foundation of China (Nos. 21275003, 21025523, 20973050), the Excellent Young Scientists Encouragement Foundation of Shandong Province (No. BS2011L015), and the Program for Changjiang Scholars and Innovative Research Team in University (PCSIRT).

[1] N. Haddour, J. Chauvin, C. Gondran, S. Cosnier, *J. Am. Chem. Soc.* **2006**, *128*, 9693–9698.
[2] M. Liang, L. Guo, *Environ. Sci. Technol.* **2007**, *41*, 658–664.
[3] M. Liang, S. Jia, S. Zhu, L. Guo, *Environ. Sci. Technol.* **2008**, *42*, 635–639.
[4] I. Willner, F. Patolsky, J. Wasserman, *Angew. Chem.* **2001**, *113*, 1913–1916; *Angew. Chem. Int. Ed.* **2001**, *40*, 1861–1864.
[5] Y. An, L. Tang, X. Jiang, H. Chen, M. Yang, L. Jin, S. Zhang, C. Wang, W. Zhang, *Chem. Eur. J.* **2010**, *16*, 14439–14446.
[6] W. Tu, J. Lei, P. Wang, H. Ju, *Chem. Eur. J.* **2011**, *17*, 9440–9447.
[7] A. Okamoto, T. Kamei, K. Tanaka, I. Saito, *J. Am. Chem. Soc.* **2004**, *126*, 14732–14733.
[8] L. Sheeney-Haj-Ichia, B. Basnar, I. Willner, *Angew. Chem.* **2005**, *117*, 80–85; *Angew. Chem. Int. Ed.* **2005**, *44*, 78–83.
[9] A. Kongkanand, R. M. Dominguez, P. V. Kamat, *Nano Lett.* **2007**, *7*, 676–680.
[10] X. Geng, L. Niu, Z. Xing, R. Song, G. Liu, M. Sun, G. Cheng, H. Zhong, Z. Liu, Z. Zhang, L. Sun, H. Xu, L. Lu, L. Liu, *Adv. Mater.* **2010**, *22*, 638–642.
[11] X. Wan, G. Long, L. Huang, Y. Chen, *Adv. Mater.* **2011**, *23*, 5342–5358.
[12] Y. Lin, K. Zhang, W. Chen, Y. Liu, Z. Geng, J. Zeng, N. Pan, L. Yan, X. Wang, J. Hou, *ACS NANO* **2010**, *4*, 3033–3038.
[13] H. Chang, X. Lv, H. Zhang, J. Li, *Electrochem. Commun.* **2010**, *12*, 483–487.
[14] C. Guo, H. Yang, Z. Sheng, Z. Lu, Q. Song, C. Li, *Angew. Chem.* **2010**, *122*, 3078–3081; *Angew. Chem. Int. Ed.* **2010**, *49*, 3014–3017.

[15] X. Zhao, S. Zhou, L. Jiang, W. Hou, Q. Shen, J. Zhu, *Chem. Eur. J.* **2012**, *18*, 4974–4981.
[16] X. Zhang, S. Li, X. Jin, S. Zhang, *Chem. Commun.* **2011**, *47*, 4929–4931.
[17] H. He, C. Gao, *Chem. Mater.* **2010**, *22*, 5054–5064.
[18] G. Wang, P. Yu, J. Xu, H. Chen, *J. Phys. Chem. C* **2009**, *113*, 11142–11148.
[19] X. Zhang, S. Li, X. Jin, X. Li, *Biosens. Bioelectron.* **2011**, *26*, 3674–3678.
[20] G. L. Wang, J. J. Xu, H. Y. Chen, S. Z. Fu, *Biosens. Bioelectron.* **2009**, *25*, 791–796.
[21] Y. Xiao, X. G. Qu, K. W. Plaxco, A. J. Heeger, *J. Am. Chem. Soc.* **2007**, *129*, 11896–11897.
[22] Y. Xiao, A. A. Lubin, B. R. Baker, K. W. Plaxco, A. Heeger, *Proc. Natl. Acad. Sci. USA* **2006**, *103*, 16677–16680.
[23] R. Tel-Vered, O. Yehezkeli, H. B. Yildiz, O. I. Wilner, I. Willner, *Angew. Chem.* **2008**, *120*, 8396–8400; *Angew. Chem. Int. Ed.* **2008**, *47*, 8272–8276.
[24] L. Sheeney-Haj-Ichia, J. Wassermann, I. Willner, *Adv. Mater.* **2002**, *14*, 1323–1326.
[25] L. Sheeney-Haj-Ichia, I. Willner, *J. Phys. Chem. B* **2002**, *106*, 13094–13097.
[26] C. Y. Zhang, H. C. Yeh, M. T. Kuroki, T. H. Wang, *Nat. Mater.* **2005**, *4*, 826–831.
[27] H. Zhou, J. Liu, J. Xu, H. Chen, *Chem. Commun.* **2011**, *47*, 8358–8360.
[28] M. M. Maye, O. Gang, M. Cotlet, *Chem. Commun.* **2010**, *46*, 6111–6113.
[29] W. Zhao, J. Wang, J. Xu, H. Chen, *Chem. Commun.* **2011**, *47*, 10990–10992.
[30] C. Gao, H. He, L. Zhou, X. Zheng, Y. Zhang, *Chem. Mater.* **2009**, *21*, 360–370.
[31] C. Harris, P. V. Kamat, *ACS NANO* **2009**, *3*, 682–690.
[32] Z. J. Jiang, D. F. Kelley, *J. Phys. Chem. C* **2011**, *115*, 4594–4602.
[33] C. J. Wang, M. Shim, P. Guyot-Sionnest, *Science* **2001**, *291*, 2390–2392.
[34] M. Graetzel, A. J. Frank, *J. Phys. Chem.* **1982**, *86*, 2964–2967.
[35] P. V. Kamat, *J. Phys. Chem. Lett.* **2012**, *3*, 663–672.
[36] R. Duan, X. Zhou, D. Xing, *Anal. Chem.* **2010**, *82*, 3099–3103.
[37] W. S. Hummers, R. E. Offeman, *J. Am. Chem. Soc.* **1958**, *80*, 1339–1339.

Received: June 22, 2012
Revised: September 18, 2012
Published online: November 5, 2012

